DOI: 10.1002/ejic.201100785

Iron Coordination Chemistry of N_2Py_2 Ligands Substituted by Carboxylic Moieties and Their Impact on Alkene Oxidation Catalysis

Frédéric Oddon,[a,b,c] Elodie Girgenti,[a,b,c] Colette Lebrun,[d] Caroline Marchi-Delapierre,[a,b,c] Jacques Pécaut,[d] and Stéphane Ménage*[a,b,c]

Keywords: Bioinorganic chemistry / Biomimetic synthesis / Asymmetric synthesis / Homogeneous catalysis / Epoxidation / Oxidation / Iron

A biomimetic approach based on Rieske dioxygenase mimics has been undertaken, which uses the tetradentate N_2Py_2 ligand platform that contains two pyridine moieties linked to a 1,2-diaminoethane or a *trans*-1,2-diaminocyclohexane backbone. Here we report the impact of the incorporation of carboxylic functionalities with the N_2Py_2 ligand on the catalytic efficiency of its Fe^{II} complexes during epoxidation with H_2O_2 as the oxidant. Five complexes have been characterized in the solid state and solution. The X-ray structure of a ferrous complex with a ligand that contains two carboxylic acid moieties shows an unexpected N_4O_3-type iron coordination sphere. Moreover, the two carboxylic groups of the ligand remain protonated and bound by its sp^2 oxygen atom. Two substitutions of the ligand with carboxylic moieties was found to be deleterious to the reactivity of the complex during alkene oxidation, whereas monosubstitution led to a slight change in the reactivity. Moreover, the catalyst built from the optically active *trans*-1,2-diaminocyclohexane backbone, $\mathbf{L^3}$, catalyzes the asymmetric epoxidation of *trans*-2-heptene with up to 17 % yield. The addition of acetic acid leads to better selectivity, enantioselectivity (38 %), and yield of the epoxidation of nonaromatic alkenes.

Introduction

The design of homogeneous catalysts for oxidation remains a great challenge. In general, the state-of-the-art consists of catalytic processes that are environmentally friendly, use inexpensive catalysts, less energy-consuming protocols, and the use of sustainable oxidants.[1] One strategy lies in mimicking metalloenzymes, by tentatively reproducing the environment of mono- or dioxygenase active sites. The targeted active site of nonheme iron oxygenases, which consists of a mononuclear iron(II) center coordinated by the so-called 2-His-1-carboxylate facial triad, has been a great source of inspiration (Figure 1).[2]

For instance Rieske dioxygenases, such as naphthalene dioxygenase (NDO), catalyze a stereospecific *cis*-dihydroxylation during the biodegradation of arenes.[2b,3] This metal-promoted biological oxidation has been particularly targeted for the development of bioinspired catalysts because they fulfill some of the requirements listed above and perform the consumption of very inert substrates. A large number of synthetic nonheme complexes has been developed as potential oxidation catalysts. Among them, catalysts based on the full reproduction of the active site of Rieske dioxygenases were found to be poorly active with H_2O_2 as the oxidant, which suggests that the presence of carboxylic groups plays an important role on the reactivity.[4] These outcomes contrast with the promising development of iron catalysts that contain tetradentate pyridine/amine (N_2Py_2) ligands with H_2O_2 as the oxidant.[5] Indeed, selective alkane functionalization has been reported with Fe[(*S*,*S*)-PDP] [(*S*,*S*)-PDP = 2-({(*S*)-2-[(*S*)-1-(pyridin-2-ylmethyl)pyrrolidin-2-yl]pyrrolidin-1-yl}methyl)pyridine][6] and [Fe(*S*,*S*,*R*)-mcpp](CF$_3$SO$_3$)$_2$ [mcpp = *N*,*N*′-dimethyl-*N*,*N*′-bis(4,5-pineno-2-picolyl)cyclohexane-1,2-diamine].[7] Alkene oxidation has also been extensively studied,[8] which revealed that the product formation, epoxide[8d–8f] or *cis*-diols,[8g,8h] can be controlled by Fe(BPMEN) [BPMEN = *N*,*N*′-dimethyl-*N*,*N*′-bis(2-pyridylmethyl)ethane-1,2-di-

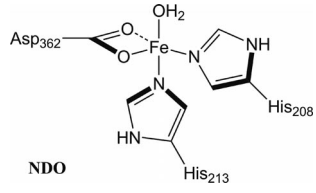

Figure 1. Representation of the catalytic iron site of NDO from *Pseudomonas* sp. NCIB 9816-4.[2b]

[a] CEA, iRTSV, Laboratoire Chimie et Biologie des Métaux, 38054 Grenoble, France
E-mail: stephane.menage@cea.fr
[b] CNRS, UMR5249, 38054 Grenoble, France
[c] Université Joseph Fourier-Grenoble I, UMR5249, 38041 Grenoble, France
[d] Laboratoire de Reconnaissance Ionique et Chimie de Coordination, LCIB (UMR-E 3 CEA/UJF-Grenoble 1), INAC/SCIB, 38054 Grenoble, France
Supporting information for this article is available on the WWW under http://dx.doi.org/10.1002/ejic.201100785.

amine],[8d] Fe(bispidine),[8e] Fe(terpyridine),[8f] Fe(TPA),[8g] or Fe(diazapyridinophane)[8h] as catalysts. A chiral N_2Py_2 ligand has led to enantioselective *cis*-dihydroxylation up to 99% *ee*, but this family of catalysts remains inefficient for enantioselective epoxidation.[9] The selectivity for epoxidation versus *cis*-dihydroxylation is partly dependent on the presence of carboxylic acids in the reaction medium, but their effect on the enantioselectivity has not been reported. This additive was proposed to control the active species by the coordination of its acid form to a η^1-Fe-peroxo species, which is a precursor of the oxidizing iron species. This helped to favor heterolytic cleavage of the O–O bond by the transfer of its proton to the distal oxygen atom of the hydroperoxo adduct. The resulting high-valent iron species epoxidized the alkene substrate with retention of configuration.[10]

Carboxylic functionalities have controversial effects on the efficiency of iron catalysts for the epoxidation of alkenes. The acidic form is of great interest for selectivity but the basic form may bind to iron, which leads to the drastic change to the electronic properties of the iron and then to a well documented loss of catalyst efficiency.[11] To circumvent this antagonistic effect, we have undertaken the design of iron catalysts using the N_2Py_2 platform [BPMEN or BPMCN, BPMCN = *N*,*N*′-bis(2-pyridylmethyl)-*N*,*N*′-dimethyl-*trans*-1,2-diaminocyclohexane],[8c] to which one or two carboxylic moieties have been introduced (Figure 2). Three new ligands have been synthesized, which differ in the number of carboxylic functional groups and/or the nature of the strap connecting the two 2-pyridylmethylamine units (Figure 2). Achieving the aim of this work relies on the design of complexes in which a carboxylic acid functional group is maintained close to the iron center in order to mimic the proposed essential catalytic transition state.[10] Ferrous, instead of ferric, complexes were targeted, which enabled us to retain the acidic form of the carboxylic moieties of the ligand as the Lewis acidity of the ferrous state is lower than that of the ferric state.

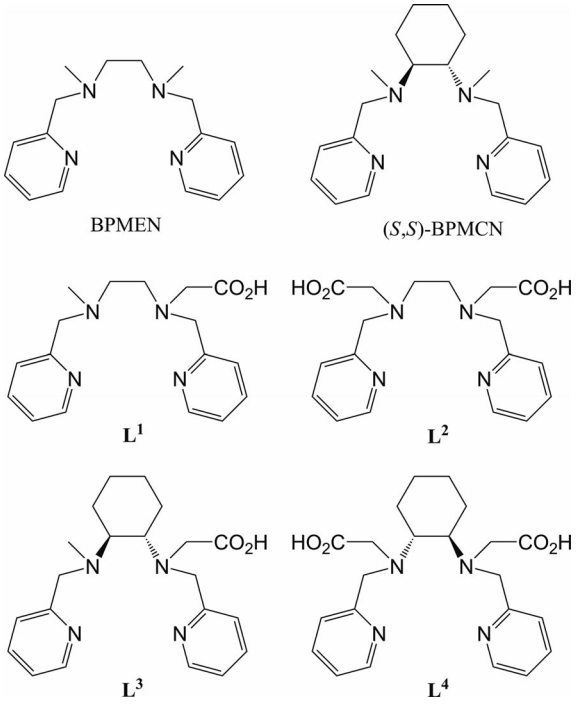

Figure 2. Representation of the ligands described in this study.

Herein we report the synthesis and characterization of five new ferrous complexes with **L**[1], **L**[2], **L**[3], and **L**[4]. The synthesis of the ferrous complexes was found to be counteranion dependent, and the complexes were formed with chloride or more weakly coordinating (ClO_4) ligands. All the complexes were characterized by various spectroscopic techniques in solution and in the solid state, which support the description of the complexes as hexa- or hepta-coordinate with bound carboxylic moieties. The complexes were tested in epoxidation catalysis, which revealed the impact of the intrinsic carboxylic group on the reactivity and enantioselectivity.

Results and Discussion

Ligands Syntheses

The synthesis of **L**[1] has already been described,[12] but as the direct insertion of a carboxymethyl arm to BPHMEN gave neither satisfactory yield, purity, or degree of protonation, we decided to insert the carboxylic moiety by a two-step route: alkylation by *tert*-butyl 2-bromoacetate followed by smooth, quantitative hydrolysis by trifluoroacetic acid (Scheme 1). The sensitivity of *tert*-butyl 2-bromoacetate precludes the use of strong bases. Because of its intrinsic basicity, BPHMEN was converted into its insoluble hydrobromide salt, which led to a limitation of the yield of 50% for the alkylation step. Nevertheless, BPHMEN·HBr was recycled. This afforded a suitable synthetic pathway that was applied to the synthesis of **L**[2], **L**[3], and **L**[4]. **L**[3] and **L**[4] incorporate the chiral *trans*-diaminocyclohexane backbone, (1*S*,2*S*) for **L**[3] and (1*R*,2*R*) for **L**[4]. The chiral diamines were used directly for the corresponding synthesis of **L**[3] and **L**[4].

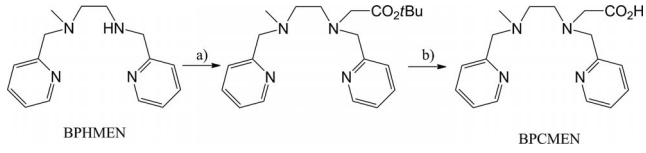

Scheme 1. a) *tert*-Butyl 2-bromoacetate, K_2CO_3, CH_3CN, 0 °C, 3 h. b) CF_3CO_2H, CH_2Cl_2, 0 °C/30 min, room temp./17 h.

Characterization of the Iron Complexes

New mononuclear complexes with potentially hexadentate **L**[2] and **L**[4] and pentadentate **L**[1] and **L**[3] ligands have been prepared. We tackled ferrous complexes as the Lewis acidity of the oxidation state is lower than that of the ferric one. Consequently, the ferric state of the complexes excludes the retention of carboxylic forms, whereas the ferrous state allows them to coexist in the same complex. To

prevent oxidation of the iron(II) complexes, they were all synthesized in a glove box. Initially, $FeCl_2$ was used to ensure a stable coordination sphere. As the formed chlorinated complexes did not precipitate in some cases, we switched to the use of $Fe(ClO_4)_2$ salts. The complexes were synthesized by reacting 1 equiv. of $Fe(ClO_4)_2$ with 1 equiv. of the ligand. When $FeCl_2$ was used, 2 equiv. of iron salt were required to maximize the yield. In some cases, powder was deposited as a function of time, otherwise diethyl ether was added to precipitate the product. All the complexes were characterized by IR, UV/Vis, and NMR spectroscopy, ESI-MS, and elemental analysis. The presence of $[FeCl_4]^{2-}$ as a counteranion for $[Fe(BPMCN)(C_3H_6O)]^{2+}$ and $[Fe(\mathbf{L^1})(C_3H_6O)]^{2+}$ was deduced from spectroscopic studies (vide infra) and supported by satisfactory elemental analyses, in which the presence of the $Cl_3Fe–O–FeCl_3$ dianion, which is the product of the air oxidation of $[FeCl_4]^{2-}$, was determined. Thanks to elemental analysis we were also able to propose stoichiometries between Fe$\mathbf{L}^n$ and the $FeCl_4$ counteranion. For example, in the case of the coordination of $\mathbf{L^4}$ to iron, the presence of an extra chloride ligand to complete the coordination sphere led to the presence of a $FeCl_4$ counteranion for two cationic species. The structures of all the complexes were deduced by comparison of their spectroscopic properties with those of the crystallographically characterized $[Fe^{II}(\mathbf{L^4})(C_3H_6O)](ClO_4)_2$.

X-ray Crystallography of $[FeII(L^4)(C_3H_6O)](ClO_4)_2$

Colorless crystals of $[Fe^{II}(\mathbf{L^4})(C_3H_6O)](ClO_4)_2$ suitable for X-ray analysis were obtained from the slow evaporation of an acetone solution of the complex in a glove box. The ORTEP representation of the cation is displayed in Figure 3. $\mathbf{L^4}$ wraps around the ferrous ion, which is heptacoordinate. The polyhedron of the iron atom is a distorted pentagonal bipyramid, in which the two nitrogen atoms from the amine moieties, the sp^2 oxygen atoms of the two carboxylic moieties of the ligand, and the acetone solvent molecule form the equatorial plane. The two pyridyl rings occupy the axial positions and have a dihedral angle of 82.4°. This unexpected N_4O_3 coordination derives from the full coordination of the ligand, of which the four nitrogen atoms are in a "*cis* α" topology and the two oxygen atoms are from the protonated form of the carboxylic ligand moieties, with an oxygen atom from a solvent molecule (this topology was based on a previously reported N_2Py_2 complex).[8c,13] The Fe–N distances range from 2.161(3) Å, which are associated with the pyridine nitrogen atoms, to 2.308(3) Å, which are associated with the amino nitrogen atoms (Table 1). These values are different to those reported for $[Fe^{II}(BPMCN)](CF_3SO_3)_2$ or $[Fe^{II}(5\text{-Me-BPMCN})](CF_3SO_3)_2$, as longer Fe–$N_{amine}$ bonds were measured in $[Fe^{II}(\mathbf{L^4})(C_3H_6O)](ClO_4)_2$, although the variation between the different Fe–N bonds (pyridine or amine functionalities) followed the same trend.[8c] The lower symmetry of $[Fe^{II}(\mathbf{L^4})(C_3H_6O)](ClO_4)_2$ and the protonation of the ligand may be responsible for the longer bonds. The Fe–O bonds are mostly long (around 2.39 Å) with the exception of that involving the acetone ligand [2.172(2) Å]. These values indicate that the carboxylic moieties of the ligand are protonated as Fe^{II}–O distances of 2.00–2.15 Å are generally reported for carboxylate ligands.[4a] The coordination mode of the carboxylic groups is rare in a discrete iron complex and has only been reported with two polynuclear species in which the carboxylic moiety connects two iron sites.[14] Finally, the Fe–O bond length in $[Fe^{II}(\mathbf{L^4})(C_3H_6O)](ClO_4)_2$ is long compared to that of another sp^2 oxygen atom–Fe^{II} bond, which involves an amido ligand.[15] Taken together, the ligand distances agree with a high-spin configuration of the ferrous ion in the solid state. Seven-coordinate iron complexes are unusual, even if iron complexes have been more extensively described than their congeners.[16] Usually, examples of ferric complexes predominate over ferrous complexes.[17]

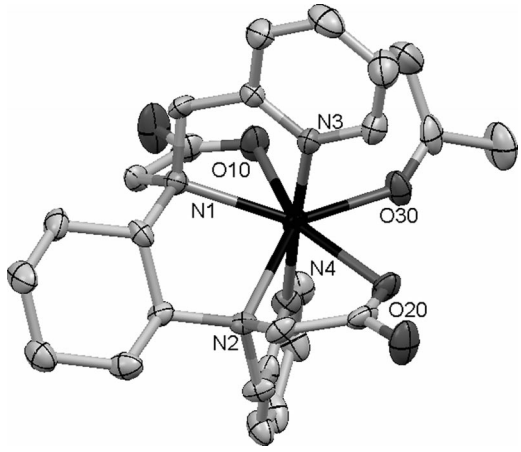

Figure 3. ORTEP representation of $[Fe^{II}(\mathbf{L^4})(C_3H_6O)]^{2+}$. Hydrogen atoms are omitted for clarity.

Table 1. Bond lengths [Å] and angles [°] for $[Fe^{II}(\mathbf{L^4})(C_3H_6O)](ClO_4)_2$.

$Fe^1–N^1$	2.308(3)	$Fe^1–N^2$	2.300(3)
$Fe^1–N^3$	2.162(3)	$Fe^1–N^4$	2.163(3)
$Fe^1–O^{10}$	2.292(2)	$Fe^1–O^{20}$	2.288(2)
$Fe^1–O^{30}$	2.172(2)		
$N^1–Fe^1–N^2$	76.96(10)	$N^1–Fe^1–N^3$	75.64(11)
$N^1–Fe^1–N^4$	106.94(10)	$N^2–Fe^1–N^3$	104.47(11)
$N^2–Fe^1–N^4$	76.50(11)	$N^3–Fe^1–N^4$	177.41(11)
$N^1–Fe^1–O^{10}$	70.27(10)	$N^1–Fe^1–O^{20}$	136.65(10)
$N^1–Fe^1–O^{30}$	142.95(10)	$N^2–Fe^1–O^{10}$	133.05(10)
$N^2–Fe^1–O^{20}$	70.80(9)	$N^2–Fe^1–O^{30}$	140.01(10)
$N^3–Fe^1–O^{10}$	99.00(11)	$N^3–Fe^1–O^{20}$	85.06(10)
$N^3–Fe^1–O^{30}$	92.27(10)	$N^4–Fe^1–O^{10}$	81.87(11)
$N^4–Fe^1–O^{20}$	93.05(10)	$N^4–Fe^1–O^{30}$	85.53(11)
$O^{10}–Fe^1–O^{20}$	152.23(8)	$O^{10}–Fe^1–O^{30}$	77.48(9)
$O^{20}–Fe^1–O^{30}$	74.90(9)		

Solid-State IR Spectroscopy

All the IR spectra of the complexes displayed characteristic features in the 1400–1750 cm^{-1} region (Figure 4). In the case of $[Fe(\mathbf{L^4})(C_3H_6O)](ClO_4)_2$, three resonances were observed, two narrow ones at 1676 and 1607 cm^{-1} that flank a broader one around 1650 cm^{-1} (Figure 4, A). The low energy peak is attributed to the asymmetric C=O vibrations of the bound acetone by comparison with literature values,[18] that at 1607 cm^{-1} to $\nu_{C=N}$ of the pyridine

rings, whereas the broad band corresponds to $\nu_{COOH_{as}}$ of the bound carboxylic groups in the complex. This energy value is between that of free ν_{COOH} (above 1750 cm^{-1}) and coordinated ν_{COO^-} (1700–1510 cm^{-1}).[19] In addition, ν_{COOH_s} is located at 1437 cm^{-1}, which implies a $\Delta(\nu_s–\nu_{as})$ of 213 cm^{-1}, a value characteristic of monodentate binding modes. In the case of $[Fe^{II}(\mathbf{L^2})](ClO_4)_2$, the same ν_{COOH} resonance was observed at 1635 cm^{-1} but no narrow peak was detected in this region, which indicates the absence of acetone as a ligand.

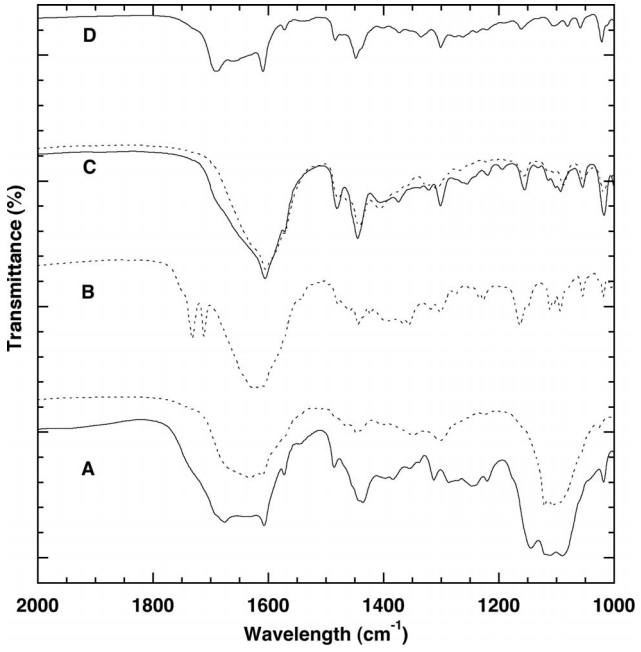

Figure 4. IR spectra of the iron complexes (solid lines for ligands with a cyclohexane moiety and dashed for ligands with an ethane moiety): **A** for $[Fe^{II}(\mathbf{L^4})(C_3H_6O)](ClO_4)_2$ and $[Fe^{II}(\mathbf{L^2})](ClO_4)_2$; **B** for $[Fe^{II}(\mathbf{L^4})(Cl)]_2(FeCl_4)$; **C** for $[Fe^{II}(\mathbf{L^3})(C_3H_6O)](FeCl_4)$ and $[Fe^{II}(\mathbf{L^1})(C_3H_6O)](FeCl_4)$; **D** for $[Fe^{III}(\mathbf{L^3})(Cl)]$ $(Fe^{III}Cl_4)$.

In the spectrum of $[Fe^{II}(\mathbf{L^4})(Cl)]_2(FeCl_4)$, two ν_{COOH} bands were observed, one at 1732 cm^{-1}, which is characteristic of a free carboxylic acid, and the other broad one around 1640 cm^{-1}, which is common to these species (Figure 4, B). The latter component was also observed in the spectra of $[Fe^{II}(\mathbf{L^3})(C_3H_6O)](FeCl_4)$ and $[Fe^{II}(\mathbf{L^1})(C_3H_6O)](FeCl_4)$ (Figure 4, C). The change in oxidation state of the metal in $[Fe^{III}(\mathbf{L^3})](FeCl_4)$ caused the slight shift of this transition to 1690 cm^{-1}, which indicates a different coordination mode or a different protonation state of the carboxylic/carboxylate moiety (Figure 4, D) (see below).

ESI-MS in Acetone

All the MS of the deoxygenated solutions of the complexes displayed a $[Fe^{II}L – H]^+$ fragment in the positive mode, which confirms the mononuclearity of the complex in solution. For $[Fe^{II}(\mathbf{L^4})(C_3H_6O)](ClO_4)_2$, a dicationic $[FeL]^{2+}$ fragment was observed as well as a fragment that contains the ClO_4 counteranion, which suggests that the carboxylic functionalities of the ligand were totally protonated in the starting solution. In the spectra of $[Fe^{II}(\mathbf{L^3})(C_3H_6O)](FeCl_4)$ and $[Fe^{II}(\mathbf{L^1})(C_3H_6O)](FeCl_4)$, a peak at m/z = 160.8 was detected in the negative mode, which was attributed to $[Fe^{II}Cl_3]^-$, a footprint of the unstable $[Fe^{II}Cl_4]^{2-}$ fragment. This was replaced in the spectrum of $[Fe^{III}(\mathbf{L^1})(Cl)](FeCl_4)$ with a peak at m/z = 197.2, which corresponds to $[Fe^{III}Cl_4]^-$. No evidence of a Cl_6Fe_2O fragment (deduced from the elemental analysis) was found.

UV/Vis Spectroscopy in Acetone

Two patterns of transitions were observed in the electronic spectra recorded under argon. First, only one transition in the near UV was observed for the perchlorate complexes, at 342 nm for $[Fe^{II}(\mathbf{L^4})(C_3H_6O)](ClO_4)_2$ and 310 nm for $[Fe^{II}(\mathbf{L^2})](ClO_4)_2$ with similar extinction coefficients in the 1500–4000 $cm^{-1}\,M^{-1}$ range, which is attributed to iron-to-nitrogen metal-to-ligand charge transfer.[20] Second, the UV/Vis spectra of $[Fe^{II}(\mathbf{L^4})(Cl)]_2(FeCl_4)$, $[Fe^{II}(\mathbf{L^3})(C_3H_6O)](FeCl_4)$, and $[Fe^{II}(\mathbf{L^1})(C_3H_6O)](FeCl_4)$ are dominated by two transitions at 360 and 310 nm with extinction coefficients of around 2000 $cm^{-1}\,M^{-1}$, which are absent in the spectra of their ClO_4^- counterparts. Interestingly, these bands were also present but more intense in the spectrum of $[Fe^{III}(\mathbf{L^1})(Cl)](FeCl_4)$, which suggests that they originate from the counteranion (Figure 5). The energy values of these transitions were found to be identical to those found in literature for the $Fe^{III}Cl_4^-$ anion.[21] However, the extinction coefficients are lower in our case, which indicates that the ferrous anion ($FeCl_4$) was partly oxidized during the measurements.

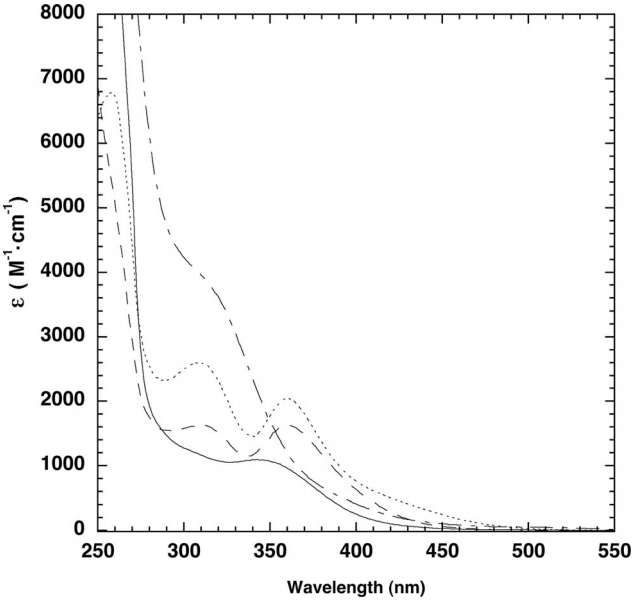

Figure 5. UV/Vis spectra of acetonitrile solutions of $[Fe^{II}(\mathbf{L^2})](ClO_4)_2$ (– - –), $[Fe^{II}(\mathbf{L^4})(C_3H_6O)](ClO_4)_2$ (– – –), $[Fe^{II}(\mathbf{L^4})(Cl)]_2(Fe^{II}Cl_4)$ (· · ·), and $[Fe^{II}(BPMCN)](Fe^{II}Cl_4)$ (- - -).

This outcome was confirmed by oxygenation of the acetonitrile solutions of the ferrous complexes (Figure 6). We observed the increase in intensity of the two transitions at 360 and 310 nm for all the chlorinated complexes to the level of the exact extinction coefficient of the $Fe^{III}Cl_4$ anion

itself. Consequently, the formation of the ferric anion arises from the oxidation of the $Fe^{II}Cl_4$, which does not have visible transitions.[21–22] The absorbance measured at 360 and 310 nm is in accordance with a ratio of 1:1 between the iron cation and its counteranion.

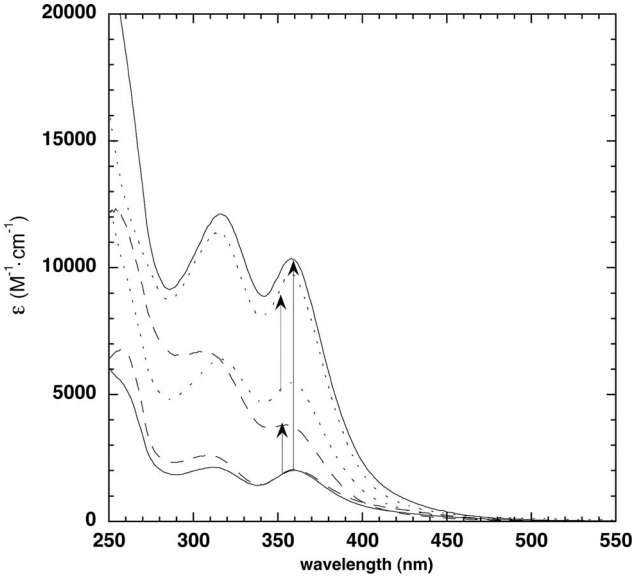

Figure 6. UV/Vis spectra of acetonitrile solutions of [Fe(BPMCN)](FeCl$_4$) ± O_2 (– – –); [Fe(**L**^{1})(C_3H_6O)](FeCl$_4$) ± O_2 (· · ·); [Fe(**L**^{4})(Cl)]$_2$(FeCl$_4$) (- - -) ± O_2. Arrows indicate the absorption changes in the presence of dioxygen.

^{1}H NMR Spectroscopy in [D_6]Acetone

^{1}H NMR spectroscopy has been shown to be a powerful tool for probing the structural and magnetic properties of iron complexes.[17,23] All the spectra (Figure 7) spanned between 170 to –40 ppm, which attests that all the complexes contain high-spin ferrous species in solution. As the resonance pattern of the NMR spectra of the complexes is reminiscent of the ligand conformation, it was possible to propose a structural topology of the ligand for most of them. First, the spectra of [Fe^{II}(**L**^{4})(C_3H_6O)](ClO_4)$_2$ and its analog [Fe^{II}(**L**^{2})](ClO_4)$_2$ consist of broad resonances above 70 ppm, which are assigned to *o*-H of the pyridine rings and the methylene proton resonances (Figure 7). The two narrow resonances that flank a broader one in the 40–60 ppm region, are attributed to *m*-H of the pyridine rings and the methylene protons. The upfield resonance at –12 ppm is tentatively assigned to *p*-protons by comparison with earlier studies.[20] The difference in the pattern of the two spectra in the 0–110 ppm region is attributed to the presence of the extra methylene protons of the strap between the two nitrogen atoms in **L**^{2} compared to **L**^{4}.

The *o*-protons are all equivalent and show a resonance at 130 ppm, which indicates that the complexes have a high symmetry. This is in agreement with the conservation of the *cis* α topology in solution. The presence of bound acetone could not unambiguously be attributed in the spectrum of [Fe^{II}(**L**^{4})(C_3H_6O)](ClO_4)$_2$, which indicates its facile exchange with a solvent molecule.

The ^{1}H NMR spectrum of [Fe^{II}(**L**^{4})(Cl)]$_2$(FeCl$_4$) was different to that of its ClO_4^- congener (Figure 7). The resonance pattern looked similar, except the loss of low-field resonances above 50 ppm, which was attributed to a change in ligand topology as *o*-H pyridine proton resonances are the most affected by the relative positions of the pyridine rings.[13] We propose that the ligand conformation was *cis* β, which leads to distinct pyridine positions in the complex structure. This leads to each *o*-H resonance becoming distinct and merging with the baseline. Moreover, the spectrum looked similar to that of the ferrous BPMCN complex, which was prepared by adding $FeCl_2$ to BPMCN in acetone. Despite the absence of X-ray structural analysis, the topology of the BPMCN complex can be deduced from an anion metathesis experiment to exchange the Cl^- ion by triflate (OTf). It has been reported that BPMCN isomers do not interconvert, which allows the structural characterization of both *cis*-α- and *cis*-β-[Fe^{II}(BPMCN)](OTf)$_2$.[13,24] Interestingly, their syntheses involved the metathesis reaction pathway with its chlorinated analog in CD_3CN.[13] Using the same procedure, the ^{1}H NMR spectroscopic pattern observed after metathesis was identical to that of β-[Fe^{II}(BPMCN)(CD_3CN)$_2$]$^{2+}$, which indicates a *cis* β topology for the BPMCN complex (Figure S3).[13,24]

The ^{1}H NMR spectrum of [Fe^{II}(**L**^{3})(C_3H_6O)](FeCl$_4$) has a complex pattern of resonances spanning between 160 and –10 ppm (Figure 7), which was attributed to the superposition of two close but distinct spectra with at least 26 proton resonances for each. It is tempting to relate this signature to the coexistence of two related topologies of the ligand. As both substituents on the amino nitrogen atoms of the ligand are different (Me versus carboxymethyl), two topologies in a similar proportion are generated only for the asymmetric geometry, i.e. *cis* β (opposite to *trans* and *cis* α). In the case of **L**^{1}, the spectrum was also very complex, which indicated that several isomers were present. In this case, the broadness of some peaks precluded an extensive interpretation of the pattern. At least we can suggest the presence of *cis* α and β conformations in nonequivalent proportions as the *trans* topology has not been observed for this type of ligand.

Based on a comparison of the solution and solid-state spectroscopic studies of all the complexes, we propose the structures of the complexes with the new ligands as depicted in Figure 8.

Catalytic Studies for Alkene Oxidations

The complexes were tested for the catalytic oxidation of several different alkenes in acetonitrile solution with H_2O_2 as the oxidant with a catalyst:substrate:H_2O_2 ratio of 1:200:300. The catalytic properties of the new complexes were compared to their BPMCN or BPMEN analogs and evaluated as a function of acetic acid or perchloric acid addition. The catalysis experiments performed in acidic conditions have been the subject of extensive studies as they determine the high selectivity for epoxides.[8d,8g]

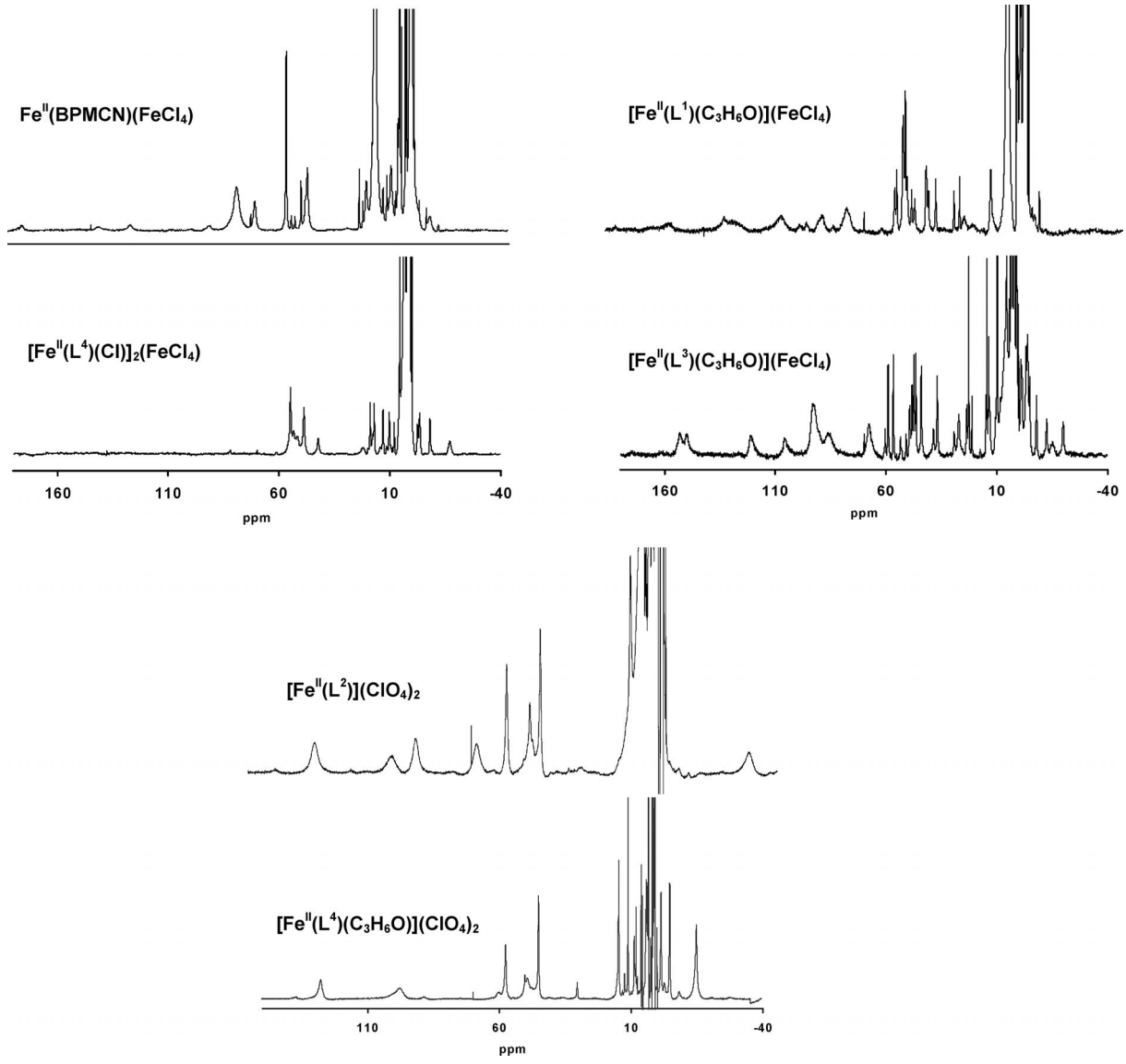

Figure 7. ^{1}H NMR spectra of iron complexes in [D_6]acetone.

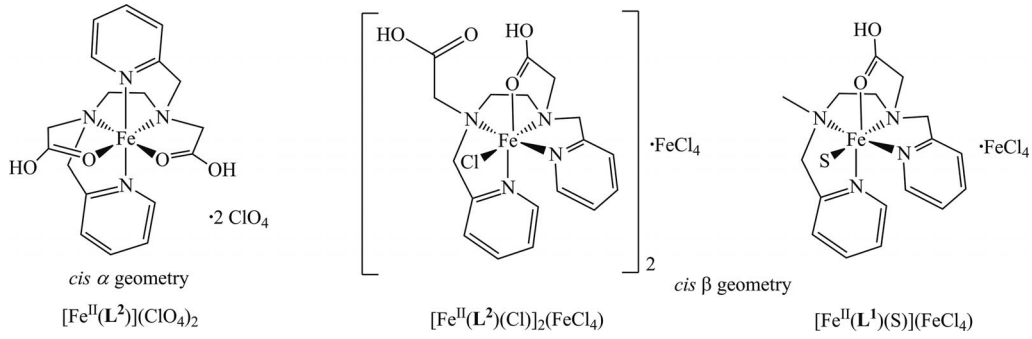

Figure 8. Proposed structures for the new iron complexes (S stands for acetone or solvent). A mixture of the *cis* α and *cis* β forms coexist in [$Fe^{II}(\mathbf{L^1})(C_3H_6O)$]($FeCl_4$).

The experiments were performed at room temperature in air. The oxidant was delivered by dropwise addition over 30 min using a syringe pump in order to reduce H_2O_2 disproportionation. The yield was measured 30 min after the end of the oxidant addition. The presence of air did not affect the yield or selectivity of the epoxidation reaction. As most complexes contain either a chloride ligand and/or an Fe(II)Cl_4 or Fe(III)Cl_4 counteranion, five equivalents of

Table 2. Cyclooctene oxidation catalyzed by [FeL]($FeCl_4$) complexes under various conditions with 0.5 mol-% catalyst.[a]

Catalyst [FeL] L	CH_3CN[a] Epoxide[b] [%]	Conv. [%]	+ 100 equiv. CH_3CO_2H Epoxide[b] [%]	Conv. [%]	CH_3CN/CH_3CO_2H 1:2 Epoxide[b] [%]	Conv. [%]	+ 1 equiv. $HClO_4$ Epoxide[b] [%]	Conv. [%]
None	0	4	1	20	1	20	–	–
$FeCl_2$	3	22	1	18	–	–	–	–
BPMEN	32	68	95	98	92	98	44	85
L¹	27	68	82	97	31	51	29	66
L²	3	37	3	37	4	37	–	–
BPMCN	56	92	64	98	63	100	38	90
L³	37	78	59	95	80	99	43	91
L⁴	1	1	1	1	4	16	–	–

[a] Ratio catalyst:substrate:H_2O_2 = 1:200:300, in CH_3CN, oxidant delivered by a syringe pump over 30 min and 30 extra minutes of stirring were allowed before GC injection. [b] Yield based on substrate consumption.

$Ag(CF_3SO_3)$ were added prior to the addition of the oxidant, which accounts for the removal of these chloride anions from the solution as they may compete with the oxidant to bind to the metal ion. This experimental requirement was supported by the total loss of epoxide formation during catalysis with these complexes in the absence of silver salts. Furthermore, $[Fe^{III}Cl_4]^-$, $Fe^{III}Cl_3$, or $Fe^{III}(ClO_4)_3$ were found to be inactive for epoxide formation under standard conditions, although a small conversion yield was measured. These control experiments guaranteed that the results obtained are attributed to the starting ferrous Fe**L***ⁿ* dication.

In the absence of either the catalyst or the oxidant, no epoxide products were detected, although the substrate was partially converted in some cases. This is particularly true when acetic acid was added to the reaction medium; up to 20% conversion was measured when 100 equiv. were added (Table 2, Column 4).

In the absence of acetic acid, $[Fe^{II}(\mathbf{L^4})(C_3H_6O)](ClO_4)_2$ and $[Fe^{II}(\mathbf{L^2})](ClO_4)_2$ were found to be quasi-inactive for cyclooctene oxidation. Conversely, reasonable epoxide yields were reached with $[Fe^{II}(\mathbf{L^3})(C_3H_6O)](FeCl_4)$ and $[Fe^{II}(\mathbf{L^1})(C_3H_6O)](FeCl_4)$ (27 and 37% yield, respectively) under the same conditions (Table 2 and Figure 9). For comparison, the BPMEN and BPMCN analogs were found to be more efficient (32[13] and 56% yield, respectively). Under our conditions, the epoxide selectivity reached 60%, although only a small amount of the corresponding diols were detected (Figure 9). As the conversion ranged from 68–92% depending on the catalyst, other secondary products were formed. ^1H NMR spectroscopic studies of the reaction media confirmed the presence of cyclooctene oxide and trace amounts of diols (less than 4%) as the major products but no other oxygenated products, such as octanedioic acid, were detected.

The presence of acetic acid increased the efficiency of the catalysts that contain **L¹** and **L³**, whereas those with **L²** and **L⁴** remained unreactive. For example, the epoxide and conversion yields increased significantly (from 37 to 80% and 78 to 100%, respectively) as acetic acid concentration increased and reached 81% selectivity with $[Fe^{II}(\mathbf{L^3})(C_3H_6O)](FeCl_4)$. By comparison, $[Fe^{II}(BPMCN)](FeCl_4)$ was unaffected under these conditions. Interestingly,

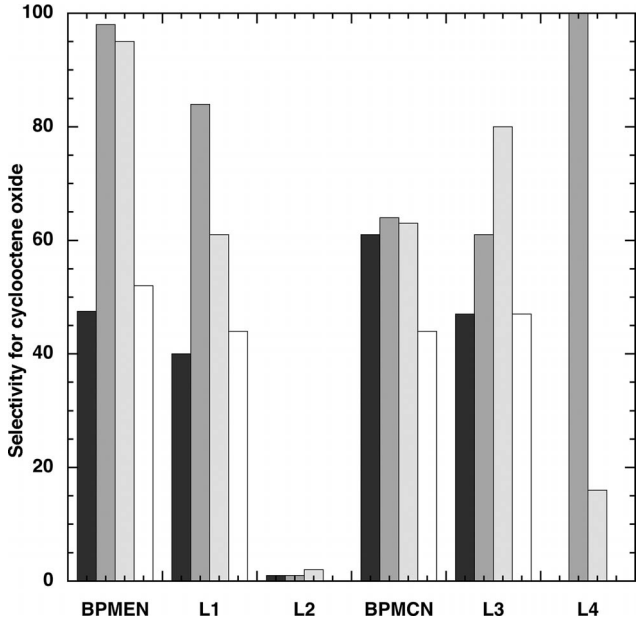

Figure 9. Selectivity for cyclooctene epoxide depending on the ligand of the iron(II) catalyst (black), in the presence of 100 equiv. acetic acid (grey), in a CH_3CN/CH_3CO_2H (1:2) solution (light grey), and in the presence of 1 equiv. of H^+ (white).

$[Fe^{II}(BPMEN)](FeCl_4)$ showed a stimulation of its reactivity (37 to 98%) with a 100% selectivity (Figure 9).[10] These results underline a difference in catalytic behavior that is related to the nature of the diamine (cyclohexanediamine vs. ethylenediamine).

The addition of 1 equiv. of $HClO_4$ was totally ineffective in stimulating the epoxidation catalysis, which implicates that protons alone are not sufficient to account for the enhancement of the reaction by acetic acid. This result suggests that acetic acid has to bind into the oxidizing species, which has been proposed earlier.[10]

The complex that contains a chiral substructure, i.e. (*S*,*S*)-cyclohexanediamine, performed enantioselective epoxidations, and the results are shown in Table 3. Interestingly, the enantioselectivity of the reaction depended on the presence of acetic acid in the reaction medium; a large increase from 15 to 34% was observed in the case of enantiomeric excess for the H_2O_2 oxidation of the *trans*-2-heptene

Table 3. Asymmetric alkene oxidation catalyzed by $[Fe^{II}L](FeCl_4)$ with 0.5 mol-% catalyst.[a]

Catalyst ([FeL]) L	CH_3CN[a] Epoxide [%]	*ee* [%]	+ 100 equiv. CH_3CO_2H Epoxide [%]	*ee* [%]	1:2 CH_3CN/CH_3CO_2H Epoxide [%]	*ee* [%]
trans-2-Heptene						
None	1	0	–	–	1	0
BPMCN	31	14	52	38	42	30
L³	18	17	29	30	40	34
trans-β-Methylstyrene						
None	3	0	3	0		
L³	7	0	6	0		
cis-β-Methylstyrene						
None	0	0	0	0		
L³	13	13	21	18		
(R)-Carvone						
None	0	0	0	0		
L³	17	5[b]	27	15[b]		

[a] Ratio catalyst:substrate:H_2O_2 = 1:200:300 in CH_3CN, oxidant delivered by a syringe pump over 30 min and 30 extra minutes of stirring were allowed before GC injection. Yield based on substrate. [b] A diastereomeric excess was measured by integration of the relevant ^1H NMR spectroscopic signals.

when 100 equiv. of acid was present. The presence of the carboxylic moiety on the ligand did not impact on the enantioselectivity of this reaction as similar values were observed with $[Fe^{II}(\mathbf{L^3})](FeCl_4)$ and $[Fe^{II}(BPMCN)](FeCl_4)$. It may suggest that the carboxylic ligand does not bind the active catalyst or does not bind in a position that affords H-bonding with the peroxide adduct. This role is devoted to the exogenous acid.

The electron richness of the substrate drastically affects the enantiomeric excess; it was found that the chiral complex was a poor catalyst for the oxidation of *cis*- or *trans*-β-methylstyrene but afforded retention of the configuration. Low but remarkable *ee* values for complexes with the N_2Py_2 ligand platform were measured,[8c] which are affected by the presence of acetic acid. Furthermore, discrimination between both diastereoisomers of the alkene by the catalyst was observed in terms of *ee* and yield. Although a racemic mixture of the corresponding epoxide was found with *trans*-(*E*)-β-methylstyrene, a noticeable enantiomeric excess was detected when *cis*-(*Z*)-β-methylstyrene was used as a substrate. Finally, benzaldehyde, propiophenone, and traces of diol were detected in less than 5% total yield, which means a poor selectivity for the epoxide. However, even if styrenes undergo competing aromatic hydroxylation reactions, which is well documented for Fe(BPMEN) and Fe(TPA),[25] such hydroxylated species were not detected here.

The selective epoxidation of (*R*)-carvone was catalyzed by $[Fe^{II}(\mathbf{L^3})(C_3H_6O)](FeCl_4)$, which proceeded by exclusive attack on the electron-rich, external C=C bond. This indicates that the oxidizing species has an electrophilic character. Moreover, the presence of acetic acid in the medium did not enhance greatly the yield of epoxide (17 versus 27% in the presence of 100 equiv. of acid) but affected the diastereomeric excess (from 5 to 15% with 100 equiv. of acetic acid). Moreover, the selectivity for the epoxide was only of 62% as two other oxygenated products were detected, one of which was definitively identified as 2-(4-methyl-5-oxocyclohex-3-en-1-yl)propanal (see Supporting Information). The other could be the alcohol analog of the latter species, which could result from Markovnikov addition of hydroxyl radicals to the double bond.[26]

Discussion

The design of complexes with carboxylic ligands was successful, thanks to the use of ferrous salts and acetone as the solvent. The new mononuclear complexes present an original property of a monodentate coordination mode of a carboxylic functionality of the ligand, which was proven by IR spectroscopy (a broad peak at 1640 cm^{-1}) for all the complexes and confirmed by the X-ray structure of $[Fe^{II}(\mathbf{L^4})(C_3H_6O)](ClO_4)_2$. The state of protonation of the carboxylic group leads to a Fe–O bond, which implies the presence of an sp^2 oxygen atom. Another characteristic of the complexes was the unexpected formation of the metallic anion $Fe^{II}Cl_4^-$, which was indirectly detected by ESI-MS and UV/Vis spectroscopy.

The geometries of the six original complexes were found to be anion dependent in acetone. The presence of a noncoordinating anion leads to the formation of *cis* α complexes, in which the pyridine rings are *trans* to each other and the carboxylic moieties are *cis* to each other (Figure 8). However, with a chloride anion, the major topology, deduced from NMR spectroscopic studies, seems to be *cis* β whatever the ligand used. We propose that the chloride ions first bind to FeL, which induces a preferred topology, before being exchanged by the carboxylic arm combined with the presence of extra coordination sites in $FeCl_2$ ($[FeCl_4]^{2-}$ is thermodynamically more stable than the expected $FeLCl_2$ complex). The geometry is also related to the lower acidity of carboxylic acids compared to HCl, which prevents deprotonation of the carboxylic acid during the synthesis. Such a phenomenon has been observed previously.[27] In one report, the degree of protonation of the ligand influenced the synthesis of the tetrachloride ferrous anion.

In terms of complex geometry, the propensity for this *cis* β topology remains puzzling but seems to be driven by the

constraints imposed by the diamine part of the ligand. A mixture of isomers was found with a more flexible diamine in an analogous complex.[24] Moreover, the cyclohexanediamine guarantees the topology in solution as it is more constrained than ethylenediamine.

In $[Fe^{II}(\mathbf{L^3})(C_3H_6O)](FeCl_4)$, the ligand in the sixth coordination position could not be unambiguously determined but Cl^- anions are excluded. We were able to compare its O_2-oxidized form with $[Fe^{III}(\mathbf{L^3})(Cl)](FeCl_4)$, which was synthesized separately. The latter complex was characterized as hexacoordinate, in which one chloride anion completed the iron coordination sphere in addition to the anionic form of the carboxylic group. Although both complexes displayed similar UV spectroscopic signatures that arise from $Fe^{III}Cl_4^-$, their ^1H NMR spectra (which were in agreement with mononuclear species) were different (Figure S5). This behavior implies a different environment around the ferric atom, which suggests that the Cl ligand is absent in the ferrous complex. We propose that the solvent, in solution, or an acetone molecule, in the solid state, is coordinated in the complex.

The catalytic properties of the original complexes were then compared to those of the BPMEN and BPMCN complexes. Initially, the use of silver salt allows the exchange of a chloride anion with acetonitrile in order to be under the previously reported catalytic conditions for the BPMEN and BPMCN complexes. The general outcome under these conditions is that the substitution of a methyl group by a carboxylic moiety on the ligand does not alter the capacity of the N_2Py_2 iron catalyst. However, two substitutions of the methyl groups by carboxylic moieties in the ligand totally poisoned the iron catalyst, which indicates that i) these moieties still bind to the oxidizing metal species or oxidant activating species and ii) they hamper the ability of the oxidant to bind. Similar results were obtained with catalysts that contain dicarboxylic ligands[4b] and, to some extent, with a system that contains one bidentate carboxylate ligand.[15] The existence of one labile site is required for catalytic activity and accounts partly for the selectivity of the alkene oxidation.[5] The high selectivity for epoxide over diol is typical of pentadentate iron catalysts, as two direct oxygen atom transfers are precluded.[28] The catalytic stimulation by acetic acid is more complicated to assess. In all cases, it had a positive effect on the conversion, the selectivity, and the epoxide yields, with the exception of the complex with BPMCN. Acetic acid has been proposed to assist the heterolytic cleavage of a transient hydroperoxo ferric intermediate, which is generally accepted as the key feature to generate the active oxidant in the cytochrome P450 mechanism.[29] In our case, proton assistance should be driven by the carboxylic moieties and/or acetic acid, which displaces the carboxylic moiety. The absence of an effect of protons alone ($HClO_4$) suggests that the acetic acid has to bind to the complex. The observed stimulation of the catalysis was modulated by the exchange between a carboxylic ligand and exogenous acetic acid in the iron coordination sphere and also depended on the orientation of carboxylic ligand towards the hydroperoxide ligand. Accordingly, the rigidity of the ligand may exclude the formation of H-bonding between the hydroperoxide and the endogenous carboxylic ligand. Moreover, this substitution process depends on the strength of the $Fe–O_{carb}$ bond. The reorganization of the coordination sphere during the process is probably more difficult for more rigid cyclohexanediamine-based complexes compared to the ethanediamine series, which generates a lower stimulating effect (Figure 9). We proposed that the easier it is for the acetic acid to bind, the higher the reactivity.

The catalyst that incorporates the optically active *trans*-1,2-diaminocyclohexane backbone into its ligand framework, i.e. complexes of $\mathbf{L^3}$, catalyzed the asymmetric epoxidation of *trans*-2-heptene with enhanced *ee* values in the presence of an external acid. Again, the presence of this intramolecular carboxylic group was not deleterious for the enantioselective control as similar *ee* values were obtained with $[Fe^{II}(BPMCN)](FeCl_4)$ and $[Fe^{II}(\mathbf{L^3})(C_3H_6O)](FeCl_4)$. The similar value obtained in the presence of acetic acid confirms that the intrinsic carboxylic group was not involved in the catalytic process (Scheme 2). The existence of an asymmetric control emphasizes the existence of a metal-based mechanism. The formation of the oxidizing species and its structure is controlled by the presence of external acetic acid. It still remains to be established if a high-valent iron species[10] is involved in the process. Further studies will be undertaken to shed light on the nature of this species in order to gain insight into the oxidation mechanism. Among the results obtained with mono- or dimeric iron catalysts for the stereoselective epoxidation of various alkenes, this is the first time that a noticeable enantiomeric excess has been obtained with a nonheme iron mononuclear catalyst and a nonelectron-rich substrate.[30]

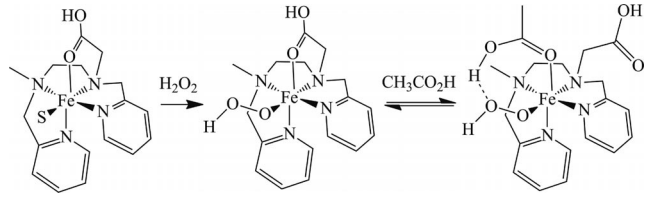

Scheme 2. Possible activation of hydrogen peroxide by the ferrous complex of $\mathbf{L^1}$ (and/or $\mathbf{L^3}$).

Conclusions

A new N_4O environment for an iron complex derived from N_2Py_2 ligands (BPMEN or BPMCN) affords a good efficiency for epoxidation, thanks to the protonation of its carboxylic group, whereas a more oxygenated N_4O_2 environment drastically affects the catalytic activity. The presence of an available, internal carboxylic functionality in the complex slightly competes with the coordination of external acetic acid, which is known to stimulate epoxidation catalysis observed with N_2Py_2 catalysts such as $[Fe(BPMCN)_2(CH_3CN)_2](CF_3SO_3)_2$. Interestingly, the stimulating effect of acetic acid combined with the weak effect of the carbox-

ylic moiety ligands was also observed for the first time for the enantioselective reaction with *trans*-2-heptene.

The presence of carboxylic functionalities may be tolerated for the design of bioinspired catalysts.

Experimental Section

General: All reagents were purchased from commercial sources and were used as received unless noted otherwise. Solvents were dried and degassed before use.

Crystallographic Studies: Data collection of $[Fe^{II}(\mathbf{L^4})(C_3H_6O)](ClO_4)_2$ were conducted with a Bruker SMART CCD system at the crystallography service of the SCIB laboratory (CEA-Grenoble). Experimental conditions for $[Fe^{II}(\mathbf{L^4})(C_3H_6O)](ClO_4)_2$: ($C_{25}H_{34}Cl_2FeN_4O_{13}$) M = 725.31 g mol^{-1}, yellow plate 0.26 × 0.17 × 0.13 mm, orthorhombic, collection wavelength 0.71073 Å; collection temperature 150(2) K, space group $P2_12_12_1$, a = 12.1116(4) Å, b = 15.7961(6) Å, c = 16.4185(6) Å, α = 90.0°, β = 90.0°, γ = 90.0°, V = 3141.11(19) Å^3, Z = 4, D_{calc} = 1.534 g cm^{-3}; Reflections collected = 10236 and 6361 independent reflections collected; $R1$ = 0.0412 [$I \leq 2\sigma(I)$]. Pertinent crystallographic data are reported in Table 1. The structure was solved by direct methods using the SHELXTL 5.03 software package. All non-hydrogen atoms were refined anisotropically. Hydrogen atoms were placed in ideal positions and refined as riding atoms with individual (or group) isotropic displacements.

CCDC-809749 contains the supplementary crystallographic data for this paper. These data can be obtained free of charge from The Cambridge Crystallographic Data Centre via www.ccdc.cam.ac.uk/data_request/cif.

Physical Studies: ^{1}H and ^{13}C NMR spectra were recorded with a Bruker Avance 300 MHz spectrometer. ^{1}H NMR chemical shifts are reported in ppm with the solvent as the internal reference. ESI-MS studies were performed with an LXQ-linear ion trap (Thermo Scientific, San Jose, CA, USA) equipped with an electrospray source in an aqueous or aqueous/acetone mixture. Electrospray full scan spectra in the range m/z = 50–2000 were obtained by infusion through fused silica tubing at 2–10 μL min^{-1}. The LXQ calibration was achieved according to the standard calibration procedure from the manufacturer (mixture of caffeine/MRFA and Ultramark 1621). The temperature of the heated capillary of the LXQ was set to 150–200 °C, and the ion spray voltage was in the range 1–3 kV. The experimental isotopic profile was compared in each case to the theoretical one. UV/Vis spectroscopic studies were carried out with a Shimadzu UV-1800 spectrophotometer. IR spectra of the complexes as KBr discs were measured with a Perkin–Elmer Spectrum 100 FT-IR spectrometer. GC was performed with a Perkin–Elmer Autosystem XL instrument with a FID detector, which used an SE 30 column coupled to a Perkin–Elmer Turbomass EI spectrometer. Enantiomeric excesses were measured by GC with a Chiraldex TA column. The values are the average of three separate samples. The diastereoisomeric excess for carvone epoxide was measured by ^{1}H NMR spectroscopy and was based on the average of the splitting of the epoxide peak at 2.68 ppm and the methyl peak at 1.30 ppm. Elemental analyses were performed by the Microanalysis Service of CNRS (Vernaison).

Synthesis of Ligands

***N*-Methyl-*N*,*N*′-bis(2-pyridylmethyl)-1,2-ethanediamine ("BPHMEN"):** Synthesized according to the method reported by Baffert et al.[12]

(1*S*,2*S*)-*N*-Methyl-*N*,*N*′-bis(2-pyridylmethyl)-1,2-cyclohexanediamine ("BPHMCN"): Synthesized by an adaptation of a previously published procedure.[31] (1*S*,2*S*)-*N*,*N*′-Bis(2-pyridylmethyl)-1,2-cyclohexanediamine (1.6 g, 5.39 mmol) was dissolved in aqueous formic acid (50 mL, 90%). Formaldehyde (9.92 mL, 25 equiv., 37%) was added and the resulting solution was stirred at 90 °C for 24 h. The mixture was cooled to 20 °C and the pH was adjusted to 12 by addition of aqueous sodium hydroxide (3 M) with constant cooling. The aqueous layer was extracted into dichloromethane, and the combined organic layers were dried with anhydrous Na_2SO_4, filtered, and evaporated to give a brown oil. Purification on a column of neutral aluminium oxide using a pentane/ethyl acetate/triethylamine mixture (50:50:1 v/v) as eluent afforded the title product (1.412 g, 85%) as a clear oil in addition to dimethylated BPMCN (15%). ^{1}H NMR (300 MHz, $CDCl_3$): BPMCN: δ = 8.55 (d, J = 4.8 Hz, 2 H, Py), 7.63 (m, 4 H, Py), 7.17 (m, 2 H, Py), 3.98 and 3.86 (d, J = 14.7 Hz, 2× 2 H, CH_2), 2.71 (m, 2 H), 2.33 (s, 6 H, 2×CH3), 2.02 (m, 2 H), 1.81 (m, 2 H), 1.26 (m, 4 H) ppm. BPHMCN: δ = 8.43 (d, J = 4.2 Hz, 2 H, Py), 7.56 (m, 3 H, Py), 7.23 (m, 1 H, Py), 7.07 (m, 2 H, Py), 3.97 (d, J = 14.1 Hz, 1 H, CH_2), 3.78 and 3.73 (ddd, J = 4.5, J = 4.8 Hz, 2 H, CH_2), 3.54 (d, J = 14.4 Hz, 1 H, CH_2), 2.43 (m, 2 H), 2.24 (m, 1 H), 2.15 (s, 3 H, CH_3), 1.89 (m, 1 H), 1.76 (m, 1 H), 1.67 (m, 1 H), 1.17 (m, 5 H) ppm.

(1*S*,2*S*)-*N*-Carboxymethyl-*N*′-methyl-*N*,*N*′-bis(2-pyridylmethyl)-1,2-cyclohexanediamine ($\mathbf{L^3}$) (General Procedure): BPHMCN (1.006 g, 3.26 mmol) was dissolved in a mixture of anhydrous MeCN (20 mL) and K_2CO_3 (720 mg, 5.22 mmol) under an inert atmosphere. *tert*-Butyl 2-bromoacetate (723 μL, 4.89 mmol) in anhydrous MeCN (20 mL) was added dropwise with a syringe over about 5 min. The reaction was then left to stir at room temperature and was monitored by TLC. Once all of the starting material had disappeared (ca. 3 h) H_2O (approx. 20 mL) was added, and the reaction mixture was extracted into dichloromethane three times. The organic phase was washed twice with brine. The combined aqueous phases were re-extracted into CH_2Cl_2. All the CH_2Cl_2 fractions were dried with Na_2SO_4 for 30 min. The drying agent was removed by filtration through a sintered funnel and the solvent was evaporated under reduced pressure. (Note: Treatment of the combined aqueous phases with NaOH followed by CH_2Cl_2 extraction led to the recovery of the starting amine with an average yield of 50%.) The crude product was then purified on a column of neutral aluminium oxide (pentane/ethyl acetate/triethylamine, 50:50:1) (732 mg, 53%). ^{1}H NMR (75 MHz, $CDCl_3$): δ = 8.43 (m, 2 H, Py), 7.77 (d, J = 7.8 Hz, 2 H, Py), 7.47–7.56 (m, 2 H, Py), 7.04–7.10 (m, 2 H, Py), 3.98 (AB, J = 12 Hz, J = 60 Hz, 2 H, CH_2CO), 3.71 (AB, J = 14.4 Hz, J = 32.4 Hz, 2 H, CH_2), 3.37 (AB, J = 16.5 Hz, J = 44.7 Hz, 2 H, CH_2), 2.6 (br., 2 H, Cy), 2.15 (s, 3 H, Me), 1.70 (br., 2 H, Cy), 1.39 (s, 9 H, *t*Bu), 1.10–1.16 (m, 4 H, Cy) ppm.

The resulting oil (732 mg, 1.73 mmol) was dissolved in CH_2Cl_2 (3 mL) under an inert atmosphere. Trifluoroacetic acid (2.53 mL, 20 equiv.) was then added slowly at 0 °C. The reaction mixture was stirred at 0 °C for 30 min. The reaction was allowed to warm to room temperature and left to stir overnight. The volume of the resulting mixture was reduced to about 4/5 under reduced pressure. The solution was then added dropwise into diethyl ether (30 mL) to precipitate the product. The resulting yellow paste was triturated several times to remove all of the trifluoroacetic acid. The remaining ether was then evaporated and left under vacuum for 5 h. The reaction was quantitative (636 mg). ^{1}H NMR (300 MHz, [D$_6$]acetone): δ = 8.65 (br., 2 H, Py), 7.92 (br., 2 H, Py), 7.61 (br., 2 H, Py), 7.46 (br., 2 H, Py), 4.89 (br., 2 H, CH_2), 4.37 (br., 2 H, CH_2), 3.53

(m, 2 H, CH_2CO), 3.01 (br., 2 H, Cy), 2.42 (m, 2 H, Cy), 1.90 (m, 2 H, Cy), 1.38 (m, 4 H, Cy) ppm.

***N*-Carboxymethyl-*N*′-methyl-*N*,*N*′-bis(2-pyridylmethyl)-1,2-ethanediamine: L¹** was synthesized using the same procedure from BPHMEN. Yield for the two steps: 50%. ^{13}C NMR (75 MHz, MeOD): δ = 172.8 (CO_2H), 157.8 (Py), 149.5 (Py), 147.9 (Py), 138.7 (Py), 137.7 (Py), 125.0 (Py), 124.4 (Py), 65.5 (CH_2Py), 58.8 (CH_2Py), 57.6 (CH_2CO), 54.2 (CH_2), 49.3 (CH_2), 40.1 (Me) ppm.

***N*,*N*′-Dicarboxymethyl-*N*,*N*′-bis(2-pyridylmethyl)-1,2-ethanediamine: L²** was synthesized using the same procedure from *N*,*N*′-bis(2-pyridylmethyl)-1,2-ethanediamine with 2.2 equiv. of *tert*-butyl 2-bromoacetate. Yield for the two steps: 41%. ^{13}C NMR (75 MHz, [D$_6$]acetone): δ = 172.1 (CO_2H), 152.3 (Py), 145.1 (Py), 142.8 (Py), 126.1 (Py), 125.3 (Py), 56.1 (CH_2Py or CH_2CO_2H), 54.2 (CH_2Py or CH_2CO_2H), 51.1 (CH_2) ppm.

***N*,*N*′-Dicarboxymethyl-(1*R*,2*R*)-*N*,*N*′-bis(2-pyridylmethyl)-1,2-cyclohexanediamine: L⁴** was synthesized using the same procedure from *N*,*N*′-bis(2-pyridylmethyl)-1,2-cyclohexanediamine with 2.2 equiv. of *tert*-butyl 2-bromoacetate. Yield for the two steps: 41%. ^{13}C NMR (75 MHz, [D$_6$]acetone): δ = 171.0 (CO_2H), 152.2 (Py), 145.5 (Py), 142.2 (Py), 125.6 (Py), 125.2 (Py), 65.2 (Cy), 62.1 (CH_2CO), 51.4 (CH_2Py), 24.2 (Cy) ppm.

Synthesis of Metal Complexes

[Fe^{II}(BPMCN)](Fe^{II}Cl$_4$) and [Fe^{II}(BPMEN)](Fe^{II}Cl$_4$): [Fe^{II}(BPMCN)](Fe^{II}Cl$_4$) and [Fe^{II}(BPMEN)](Fe^{II}Cl$_4$) were synthesized according to a literature procedure.[13,32] ESI-MS (acetone): *m*/*z* (%) = 162.8 (100) [Fe^{II}Cl$_3$]$^-$.

[Fe^{II}(L³)(C$_3$H$_6$O)](Fe^{II}Cl$_4$) (General Procedure): In a glove box, **L³** (102.9 mg, 0.28 mmol) was dissolved in acetone (approx. 10 mL). Fe^{II}Cl$_2$ (55.9 mg, 0.28 mmol) was added, and the mixture was left to stir for 30 min. The complex precipitated out within 5 min. More solid appeared on addition of diethyl ether. The complex presented as a yellow solid (60%). ^1H NMR (300 MHz, [D$_6$]acetone): δ = 153.1, 149.9, 121.0, 105.6, 93.1, 86.1, 67.6, 60.5, 59.1, 56.8, 53.4, 51.1, 49.4, 48.3, 47.4, 46.6, 44.1, 38.6, 36.9, 29.4, 27.2, 23.6, 22.7, 21.3, 15.0, 14.5, 13.8, 9.89, 6.42, 5.25, 2.20, 1.13, –0.11, –1.54, –3.11, –3.69, –4.80, –7.88, –12.5, –15.1, –19.8 ppm. IR (KBr): $\tilde{\nu}$ = 3442 (ν_{OH}), 2926 (ν_{CH}), 1638 ($\nu_{C=O_{as}}$), 1443 ($\nu_{C=O_s}$) cm^{-1}. ESI-MS (acetone): *m*/*z* (%) = 423.4 (100) [L – H + Fe^{II}]$^+$, 459.2 (24) [L + Cl + Fe^{II}], 481.3 (83) [L – H + Cl + Na + Fe^{II}]. Because of its sensitivity to oxygen, the Fe^{II}Cl$_4$ counterion was transformed to the more stable dimer Cl$_3$Fe^{II}OHFe^{II}Cl$_3$ during sample preparation for elemental analysis. [Fe^{II}(**L³**)(C$_3$H$_6$O)](Cl$_3$Fe^{II}OHFe^{II}Cl$_3$)$_2$·1H$_2$O: $C_{24}H_{40}Cl_{12}Fe_5N_4O_7$ (1201.27): calcd. C 24.35, H 3.16, N 4.73; found C 24.87, H 3.58, N 4.41.

[Fe^{II}(L¹)(C$_3$H$_6$O)](Fe^{II}Cl$_4$): The same procedure was used as described above; yield 74%. ^1H NMR (300 MHz, [D$_6$]acetone): δ = 161.5, 152.8, 129.6, 105.4, 97.5, 94.5, 88.1, 77.3, 57.1, 56.1, 53.5, 52.6, 51.8, 50.0, 48.6, 43.7, 42.8, 39.7, 31.9, 29.5, 27.7, 16.4, 9.27, 5.46, 5.26, 5.01, 2.99, 0.56, –1.14, –2.52, –4.23, –17.4 ppm. IR (KBr): $\tilde{\nu}$ = 3400 (ν_{OH}), 1620 ($\nu_{C=O_{as}}$), 1609 ($\nu_{C=N}$), 1445 ($\nu_{C=O_s}$) cm^{-1}. ESI-MS (acetone): *m*/*z* (%) = 369.3 (100) [L – H + Fe^{II}]$^+$. [Fe^{II}(L¹)(C$_3$H$_6$O)](Cl$_3$Fe^{II}OFe^{II}Cl$_3$)·2H$_2$O: $C_{20}H_{32}Cl_6Fe_3N_4O_6$ (804.76): calcd. C 29.85, H 4.01, Cl 26.43, Fe 20.82, N 6.96; found C 29.22, H 3.38, Cl 28.39, Fe 19.62, N 7.95.

[Fe^{II}(L⁴)(Cl)]$_2$(Fe^{II}Cl$_4$): The same procedure was used as described above; yield 59%. ^1H NMR (300 MHz, [D$_6$]acetone): δ = 54.8, 53.2, 51.6 and 42.3 (CH_2, H_m and H_m'), 21.5, 18.9, 17.0, 13.6, 13.2, 10.7, 10.3 and 8.14 (CH_2), –3.53, –3.43, –8.08, –17.2 (CH_2 and H_p) ppm. IR (KBr): $\tilde{\nu}$ = 3392 (ν_{OH}), 1647 ($\nu_{C=O_{as}}$), 1607 ($\nu_{C=N}$), 1444 ($\nu_{C=O_s}$) cm^{-1}. ESI-MS (acetone): *m*/*z* = 467.4 (100) [L – H + Fe^{II}]$^+$, 933.4 (83) [2(L – H) – H + 2Fe^{II}]$^+$, 955.4 (34) [2(L – 2H) + Na + 2Fe^{II}]$^+$. [Fe^{II}(**L⁴**)(Cl)]$_2$(Fe^{II}Cl$_4$): $C_{44}H_{56}Cl_6Fe_3N_8O$ (1093.24): calcd. C 43.85, H 4.68, N 9.30; found C 43.62, H 4.97, N 9.15.

[Fe^{II}(L⁴)(C$_3$H$_6$O)](ClO$_4$)$_2$: In a glove box, **L⁴** (105.3 mg, 0.26 mmol) was dissolved in acetone (approx. 10 mL). Fe^{II}(ClO$_4$)$_2$ (65.1 mg, 0.26 mmol) was added, and the mixture was stirred for 30 min. Addition of diethyl ether (5 mL) to the yellow-green solution led to the precipitation of the complex The product was washed with diethyl ether and dried under vacuum to afford a yellowish solid (43%). ^1H NMR (300 MHz, [D$_6$]Acetone): δ = 127.9 (H_o), 97.9 and 88.7 (CH_2), 60.3, 57.7, 49.4 and 45.2 (H_m, H_m' and CH_2), 14.8 (H_p), –4.63, –8.20 and –14.7 (CH_2) ppm. IR (KBr): $\tilde{\nu}$ = 3400 (ν_{OH}), 1640 ($\nu_{C=O_{as}}$), 1608 ($\nu_{C=N}$), 1436 ($\nu_{C=O_s}$), 1144, 1090 and 1111 (ν_{ClO}) cm^{-1}. ESI-MS (acetone): *m*/*z* (%) = 234.2 (64) [L + Fe^{II}]$^{2+}$/2, 467.3 (100) [L – H + Fe^{II}]$^+$, 566.8 (7) [L + ClO$_4$ + Fe^{II}]$^+$. [Fe^{II}(**L⁴**)(C$_3$H$_6$O)](ClO$_4$)$_2$·(H$_2$O): $C_{25}H_{36}Cl_2FeN_4O_{14}$ (743.33): calcd. C 40.40, H 4.84, Fe 7.50, N 7.54; found C 40.60, H 4.93, Fe 6.50, N 7.49.

[Fe^{II}(L²)](ClO$_4$)$_2$: The same procedure was used as described above; yield 51%. ^1H NMR (300 MHz, [D$_6$]Acetone): δ = 125.9 (H_o), 98.3, 89.8 and 67.9 (CH_2), 57.4, 49.1 and 45.3 (H_m, H_m' and CH_2), 13.0 (H_p), –29.7 (H_p or CH_2) ppm. IR (KBr): $\tilde{\nu}$ = 3436 (ν_{OH}), 1622 ($\nu_{C=O_{as}}$), 1611 ($\nu_{C=N}$), 1447 ($\nu_{C=O_s}$), 1121 and 1108 (ν_{ClO}) cm^{-1}. ESI-MS (acetone): *m*/*z* (%) = 448.2 (100) [L – H + Cl + Fe^{III}]$^+$, 413.3 (46) [L – H + Fe^{II}]$^+$. [Fe^{II}(**L²**)](ClO$_4$)$_2$: $C_{18}H_{22}Cl_2FeN_4O_{12}$ (613.14): calcd. C 35.26, H 3.62, Cl 11.56, Fe 9.11, N 9.14; found C 35.63, H 3.93, Cl 10.40, Fe 9.44, N 8.93.

[Fe^{III}(L⁴)(Cl)](Fe^{III}Cl$_4$): Under air, **L⁴** (63 mg, 0.15 mmol) was dissolved in acetone (approx. 6 mL). Fe^{III}Cl$_3$·6H$_2$O (41 mg, 0.15 mmol) dissolved in acetone (approx. 2 mL) was added dropwise to afford an orange solution. After 2 h of stirring, the complex was precipitated by the addition of diethyl ether (approx. 10 mL). The product was washed with diethyl ether and dried under vacuum to give a yellow solid (44%). ^1H NMR (300 MHz, MeOD): δ = 76.7, 58.9, 26.7 and –18.6 ppm. IR (KBr): $\tilde{\nu}$ = 3412 (ν_{OH}), 2936 (ν_{CH}), 1643 ($\nu_{C=O_{as}}$), 1445 ($\nu_{C=O_s}$) cm^{-1}. ESI-MS (MeOH): *m*/*z* (%) = 466.3 (100) [L – 2H + Fe^{III}]$^+$, 502.2 (5) [L – H + Cl + Fe^{III}]$^+$. [Fe^{III}(**L⁴**)(Cl)](Fe^{III}Cl$_4$): $C_{21}H_{30}Cl_5Fe_2N_4O_4$ (691.45): calcd. C 36.48, H 4.37, Fe 16.15, Cl 25.64, N 8.10; found C 36.89, H 4.13, Fe 16.45, Cl 26.02, N 8.04.

Reaction Conditions for Catalysis Experiments: A H_2O_2 solution in CH_3CN (150 μL, 2.0 M, diluted from a 50% H_2O_2 solution) was delivered by syringe pump over 30 min at room temperature in air (or added all at once) to a vigorously stirred CH_3CN solution (850 μL) that contained catalyst (1 μmol), substrate (200 μmol), and of $AgCF_3SO_3$ (4.5 μmol). The final concentrations were 1 mM iron catalyst, 300 mM H_2O_2, and 200 mM substrate. The solution was stirred for another 30 min after the H_2O_2 addition. These experiments were carried out at room temperature with a variable amount of acetic acid (100 equiv. of CH_3COOH or a 1:2 mixture CH_3CN/CH_3COOH) or with $HClO_4$ (1 mM). A benzophenone solution in CH_2Cl_2 (20 μL, 1 M) was added as an internal reference to the samples before GC analysis. The products were identified by comparison of their GC retention times and GC–MS with those of authentic compounds and ^1H NMR spectroscopy. For NMR spectroscopic characterization, the solution was washed with saturated $NaHCO_3$ solution, and the organic layer was dried with Na_2SO_4 then evaporated under reduced pressure before analysis. All experiments were run at least in duplicate, and the reported data are the average of these reactions. See Supporting Information for product identification for (*R*)-carvone oxidation.

Supporting Information (see footnote on the first page of this article): Complex characterization (ESI-MS, NMR spectra in the presence of O_2 or triflate), characterization of the products of (*R*)-carvone oxidation.

Acknowledgments

This research was supported by the Agence Nationale pour la Recherche (ANR) (H:AMAC Project ANR-08-CP2D-12) and by the Région Rhône-Alpes Cible.

[1] P. T. Anastas, M. M. Kirchhoff, *Acc. Chem. Res.* **2002**, *35*, 686–694.
[2] a) E. G. Kovaleva, J. D. Lipscomb, *Science* **2007**, *316*, 453–457; b) B. Kauppi, K. Lee, E. Carredano, R. E. Parales, D. T. Gibson, H. Eklund, S. Ramaswamy, *Structure* **1998**, *6*, 571–586.
[3] S. M. Resnick, K. Lee, D. T. Gibson, *J. Ind. Microbiol. Biotechnol.* **1996**, *17*, 438–457.
[4] a) P. D. Oldenburg, C. Y. Ke, A. A. Tipton, A. A. Shteinman, L. Que, *Angew. Chem.* **2006**, *118*, 8143; *Angew. Chem. Int. Ed.* **2006**, *45*, 7975–7978; b) P. C. A. Bruijnincx, I. L. C. Buurmans, S. Gosiewska, M. A. H. Moelands, M. Lutz, A. L. Spek, G. van Koten, R. J. M. K. Gebbink, *Chem. Eur. J.* **2008**, *14*, 1228–1237; c) P. D. Oldenburg, Y. Feng, I. Pryjomska-Ray, D. Ness, L. Que, *J. Am. Chem. Soc.* **2010**, *132*, 17713–17723.
[5] L. Que, W. B. Tolman, *Nature* **2008**, *455*, 333–340.
[6] M. S. Chen, M. C. White, *Science* **2007**, *318*, 783–787.
[7] L. Gomez, I. Garcia-Bosch, A. Company, J. Benet-Buchholz, A. Polo, X. Sala, X. Ribas, M. Costas, *Angew. Chem.* **2009**, *121*, 5830; *Angew. Chem. Int. Ed.* **2009**, *48*, 5720–5723.
[8] a) M. Klopstra, G. Roelfes, R. Hage, R. M. Kellogg, B. L. Feringa, *Eur. J. Inorg. Chem.* **2004**, 846–856; b) A. Company, L. Gomez, X. Fontrodona, X. Ribas, M. Costas, *Chem. Eur. J.* **2008**, *14*, 5727–5731; c) M. Costas, A. K. Tipton, K. Chen, D. H. Jo, L. Que, *J. Am. Chem. Soc.* **2001**, *123*, 6722–6723; d) M. C. White, A. G. Doyle, E. N. Jacobsen, *J. Am. Chem. Soc.* **2001**, *123*, 7194–7195; e) M. R. Bukowski, P. Comba, A. Lienke, C. Limberg, C. L. de Laorden, R. Mas-Balleste, M. Merz, L. Que, *Angew. Chem.* **2006**, *118*, 3524; *Angew. Chem. Int. Ed.* **2006**, *45*, 3446–3449; f) P. Liu, E. L. M. Wong, A. W. H. Yuen, C. M. Che, *Org. Lett.* **2008**, *10*, 3275–3278; g) K. Chen, M. Costas, J. H. Kim, A. K. Tipton, L. Que, *J. Am. Chem. Soc.* **2002**, *124*, 3026–3035; h) T. W. S. Chow, E. L. M. Wong, Z. Guo, Y. G. Liu, J. S. Huang, C. M. Che, *J. Am. Chem. Soc.* **2010**, *132*, 13229–13239.
[9] K. Suzuki, P. D. Oldenburg, L. Que, *Angew. Chem.* **2008**, *120*, 1913; *Angew. Chem. Int. Ed.* **2008**, *47*, 1887–1889.
[10] R. Mas-Balleste, L. Que, *J. Am. Chem. Soc.* **2007**, *129*, 15964–15972.
[11] M. Costas, K. Chen, L. Que, *Coord. Chem. Rev.* **2000**, *200*, 517–544.
[12] C. Baffert, M. N. Collomb, A. Deronzier, S. Kjaergaard-Knudsen, J. M. Latour, K. H. Lund, C. J. McKenzie, M. Mortensen, L. Nielsen, N. Thorup, *Dalton Trans.* **2003**, 1765–1772.
[13] M. Costas, L. Que, *Angew. Chem.* **2002**, *114*, 2283; *Angew. Chem. Int. Ed.* **2002**, *41*, 2179–2181.
[14] a) Y. Xu, R. H. Wang, B. Y. Lou, L. Han, M. C. Hong, *Acta Crystallogr., Sect. C: Cryst. Struct. Commun.* **2004**, *60*, M296–M298; b) F. Marchetti, B. Melai, G. Pampaloni, S. Zacchini, *Inorg. Chem.* **2007**, *46*, 3378–3384.
[15] P. D. Oldenburg, A. A. Shteinman, L. Que, *J. Am. Chem. Soc.* **2005**, *127*, 15672–15673.
[16] D. Casanova, P. Alemany, J. M. Bofill, S. Alvarez, *Chem. Eur. J.* **2003**, *9*, 1281–1295.
[17] D. G. Lonnon, G. E. Ball, I. Taylor, D. C. Craig, S. B. Colbran, *Inorg. Chem.* **2009**, *48*, 4863–4872.
[18] I. Perelygin, M. Klimchuk, *J. Appl. Spectrosc.* **1974**, *20*, 687–688.
[19] K. Nakamoto, *Infrared and Raman Spectroscopy of Inorganic and Coordination Compounds*, 4th ed., Wiley, New York, **1986**, p. 231–233.
[20] Y. Mekmouche, S. Menage, J. Pecaut, C. Lebrun, L. Reilly, V. Schuenemann, A. Trautwein, M. Fontecave, *Eur. J. Inorg. Chem.* **2004**, 3163–3171.
[21] A. P. Ginsberg, M. B. Robin, *Inorg. Chem.* **1963**, *2*, 817–822.
[22] P. A. Shapley, W. S. Bigham, M. T. Hay, *Inorg. Chim. Acta* **2003**, *345*, 255–260.
[23] S. Menage, J. M. Vincent, C. Lambeaux, G. Chottard, A. Grand, M. Fontecave, *Inorg. Chem.* **1993**, *32*, 4766–4773.
[24] R. Mas-Balleste, M. Costas, T. van den Berg, L. Que, *Chem. Eur. J.* **2006**, *12*, 7489–7500.
[25] a) O. V. Makhlynets, P. Das, S. Taktak, M. Flook, R. Mas-Balleste, E. V. Rybak-Akimova, L. Que, *Chem. Eur. J.* **2009**, *15*, 13171–13180; b) N. Y. Oh, M. S. Seo, M. H. Lim, M. B. Consugar, M. J. Park, J. U. Rohde, J. H. Han, K. M. Kim, J. Kim, L. Que, W. Nam, *Chem. Commun.* **2005**, 5644–5646; c) S. Taktak, M. Flook, B. M. Foxman, L. Que, E. V. Rybak-Akimova, R. Akimova, *Chem. Commun.* **2005**, 5301–5303.
[26] R. Rinaldi, H. F. N. de Oliveira, H. Schumann, U. Schuchardt, *J. Mol. Catal. A* **2009**, *307*, 1–8.
[27] a) P. Pelagatti, A. Bacchi, M. Balordi, A. Caneschi, M. Giannetto, C. Pelizzi, L. Gonsalvi, M. Peruzzini, F. Ugozzoli, *Eur. J. Inorg. Chem.* **2007**, 162–171; b) M. Kim, Y. U. Kim, J. H. Han, *Polyhedron* **2007**, *26*, 4003–4008.
[28] K. Chen, M. Costas, J. L. Que, *J. Chem. Soc., Dalton Trans.* **2002**, 672–679.
[29] a) B. S. Lane, K. Burgess, *Chem. Rev.* **2003**, *103*, 2457–2473; b) S. Taktak, W. H. Ye, A. M. Herrera, E. V. Rybak-Akimova, *Inorg. Chem.* **2007**, *46*, 2929–2942.
[30] a) Q. H. Xia, H. Q. Ge, C. P. Ye, Z. M. Liu, K. X. Su, *Chem. Rev.* **2005**, *105*, 1603–1662; b) H. L. Yeung, K. C. Sham, C. S. Tsang, T. C. Lau, H. L. Kwong, *Chem. Commun.* **2008**, 3801–3803; c) Y. Nishikawa, H. Yamamoto, *J. Am. Chem. Soc.* **2011**, *133*, 8432–8435; d) C. Marchi-Delapierre, A. Jorge-Robin, A. Thibon, S. Menage, *Chem. Commun.* **2007**, 1166–1168; e) F. G. Gelalcha, B. Bitterlich, G. Anilkumar, M. K. Tse, M. Beller, *Angew. Chem.* **2007**, *119*, 7431; *Angew. Chem. Int. Ed.* **2007**, *46*, 7293–7296.
[31] T. Soundiressane, S. Selvakumar, S. Menage, O. Hamelin, M. Fontecave, A. P. Singh, *J. Mol. Catal. A* **2007**, *270*, 132–143.
[32] K. Chen, L. Que, *Chem. Commun.* **1999**, 1375–1376.

Received: July 27, 2011
Published Online: December 2, 2011

